



Assessing internal changes in the future structure of Dry-Hot compound events. The case of the Pyrenees

Marc Lemus-Canovas¹, Joan Albert Lopez-Bustins¹

¹Climatology Group, Department of Geography, University of Barcelona, Barcelona, 08001, Spain

5 *Correspondence to:* Marc Lemus-Canovas (mlemus@ub.edu)

Abstract. Impacts upon vulnerable areas such as mountain ranges may become greater under a future scenario of adverse climatic conditions. In this sense, the concurrence of long dry spells and extremely hot temperatures can induce environmental risks such as wildfires, crop yield losses or other problems, the consequences of which could be much more serious than if these events were to occur separately in time (e.g. only long dry spells). The present study attempts to address recent and future changes in the following dimensions: duration (D), magnitude (M) and extreme magnitude (EM) of compound Dry-Hot events in the Pyrenees. The analysis focuses upon changes in the extremely long dry spells and extremely high temperatures that occur within these dry periods, in order to estimate whether the internal structure of the compound event underwent a change in the observed period (1981-2015) and whether it will change in the future (2011-2100) under intermediate (RCP4.5) and high (RCP8.5) emission scenarios. To this end, we quantified the changes in the temporal trends of such events, as well as changes in the bivariate probability density functions for the main Pyrenean regions. The results showed that to date the risk of the compound event has increased by only one dimension –magnitude (including extreme magnitude) – during the last few decades. In relation to the future, increased in risk was found to be associated with an increase both in the magnitude and the duration (extremely long dry spells) of the compound event, mainly in the eastern and southern regions of the Pyrenees.

20

1. Introduction

Research on dry spells or droughts, as well as extreme heat events (i.e. heat waves) is habitually based upon an individual focus, and the compound nature of such events is often neglected. In this sense, in the case of spells (whether dry or wet), several studies have examined the duration thereof and have quantified the trends of such events in different regions of the world (Martin-Vide and Gomez, 1999; Zolina et al., 2013; Singh et al., 2014); however, the thermal component of these episodes has not been addressed therein. Similarly, we found different studies on temperature extremes that did not evaluate the effect of duration of such extremes (Diffenbaugh and Ashfaq 2010; Fonseca et al., 2016; Salameh et al., 2019). In general terms, the indices proposed by the Expert Team on Climate Change Detection and Indices (ETCCDI) do not involve analyzing events in a composite manner, a shortcoming that can result in underestimation of risk (Zscheischler et al., 2018).



30 As mentioned above, compound analysis of events enables us to estimate the real risk induced by the simultaneous
occurrence of several climatic variables; this is of particular interest in fragile and vulnerable areas, such as mountain ranges,
in a context of anthropogenic climate change. In this sense, the area of the Pyrenees (Fig. 1), a transboundary area between
three countries (Andorra, France and Spain), possesses a great wealth of natural resources and a high level of biodiversity.
However, Some studies have already addressed the initial impacts of the warming observed in this region, particularly in
35 relation to the decline of mountain forests (Camarero 2017). In addition, more frequent dry periods and droughts have also
led to the defoliation of silver fir (*Abies alba*) forests in this region (Gazol et al., 2020). There is therefore an urgent need for
a compound analysis of extreme dry spells and extreme warm temperature events, i.e. the combination of duration (D) and
magnitude (M), as conceptualized in Manning et al., (2019), in order to ascertain whether these compound events will be
more widespread in the future and whether they pose other risks such as wildfires or crop yield losses.

40 As for the compound analysis of Dry-Hot events, previous studies have highlighted an increase in the frequency and spatial
scope of such events in recent years in several areas such as the US (Mazdiyasi and AghaKouchak 2015), India (Sharma
and Mujumdar 2017) or China (Wu et al., 2019), although in Europe the magnitude (temperature) of these events was
revealed to have greater weight than their duration (dry spells) (Manning et al., 2019). Several recently published studies
focus mainly on the changes observed in these compound events (Wu et al., 2019; Hao et al., 2019; Manning et al., 2019).
45 However, fewer analyses have employed future projections to assess the risk posed by the occurrence of compound events
(Zscheischler and Seneviratne 2017; Lu et al., 2018; Wu et al., 2020). Zscheischler and Seneviratne (2017) used Copula's
method to evaluate changes in the probability of future Dry-Hot compound events; they employed the Coupled Model
Intercomparison Project (CMIP5) simulations to show an increase in the probability of these events in most regions of the
world. Previous research has therefore highlighted a general increase in this kind of events, but they have neglected to
50 separately address the importance of the variables contributing to such compound events. Thus, the present study will
attempt to account for the influence of the variables giving rise to Dry-Hot compound events.

Herein we analyze the observed and projected changes in Dry-Hot compound events, understanding these as the combination
of extremely long dry periods and extremely high temperatures within these periods. The main objectives of our paper are: 1)
to define the duration (D), magnitude (M) and extreme magnitude (EM) of events; 2) to estimate the observed regional
55 trends of the variables at play in the compound event; 3) to project the future trends of such compound events, under
different Representative Concentration Pathways (RCPs), in order to determine future changes in the weights of each
variable involved in the compound event. As an intermediate and essential step between tasks 2 and 3, we will apply and
evaluate a bias correction in relation to the historical simulations.

Section 2 describes the data collection method used in our study, including the observed and simulated data, the
60 methodology employed to obtain the regionalized series of the Pyrenees, the criteria used to define each event, and the bias
correction method and the assessment thereof. In section 3, we present the exploratory analysis of the variables constituting
the compound event, as well as the observed trends in the main regions of the study area defined in section 2. In section 4,
we perform an exhaustive evaluation of the effects of the bias correction method applied to the series simulated by the



65 climate models. Subsequently, in section 5, we analyze the results of the projection of the variables described in section 2
with the use of different RCPs, in order to estimate changes in the internal structure of the Hot-Dry compound event. Finally,
section 6 presents the discussion of the results, and section 7 some brief conclusions.

2. Data and methods

2.1 Observed and projected data

70 The accumulated daily precipitation and maximum daily temperature of the spring and summer seasons (MAM and JJA)
were extracted from the database of the CLIMPY project (Characterization of the evolution of climate and provision of
information for adaptation in the Pyrenees); this is a transboundary initiative whose objective is to perform a detailed
analysis of recent trends in temperature, precipitation and snow cover in the Pyrenees, as well as the future projection thereof
(Cuadrat et al., 2020). These two variables were provided in a 1x1 km high-resolution grid, for the 1981-2015 period, and
75 fed by 1,343 weather stations located in Andorra, France and Spain; the grid was built following the quality control,
reconstruction and gridding processes according to Serrano-Notivoli et al., (2017 and 2019). We focused on spring and
summer, as spring can constitute the precursor of summer wildfires, and is a season prone to crop yield losses, etc. We also
centered our attention on summer, as this is the hottest and driest time of year in the area and is the most critical period for
the occurrence of the above mentioned environmental risks.

80 For the climate simulation projections, six climate models were obtained from different Regional Climate Models (RCMs),
which were nested in different General Circulation Models (GCMs) AND computed over Europe (Table 1), within the
framework of the Coordinated Regional Climate Downscaling Experiment (EURO-CORDEX) (Jacob et al., 2014). These
gridded projections cover all of Europe with a spatial resolution of 0.11° in latitude and longitude (~12 km) for the 1981-
2005 (historical experiment) and 2006-2100 (RCPs scenarios) periods. The models chosen were those that provided
sufficient data for such a study, and which had been used and validated in previous studies (Jacob et al., 2014). Additionally,
85 the RCPs used were the 4.5 –stabilization without overshoot pathway to 4.5 W/m² (~650 ppm CO₂) stabilization after 2100
(Wise et al., 2009)– and the 8.5 –rising radiative forcing pathway leading to 8.5 W/m² (~1370 ppm CO₂) by 2100 (Riahi et
al., 2007)–. Herein we did not employ the gridded data but rather the cell closest to the centroid of each region (Fig. 1).



Table 1. EURO-CORDEX climatic models used and their characteristics. Source: Copernicus Climate Change Service (<https://cds.climate.copernicus.eu/cdsapp#!/home>, last accessed 10 July 2020).

Model	Institute	GCM	RCM
1	CNRM	CNRM-CM5	ALADIN-63
2	CNRM	CNRM-CM5	RACMO22E
3	DMI	NCC-NorESM1-M	DMI-HIRHAM5
4	KNMI	EC-EARTH	RACMO22E
5	SMHI	IPSL-CM5A-MR	RCA4
6	SMHI	MPI-ESM-LR	RCA4

95

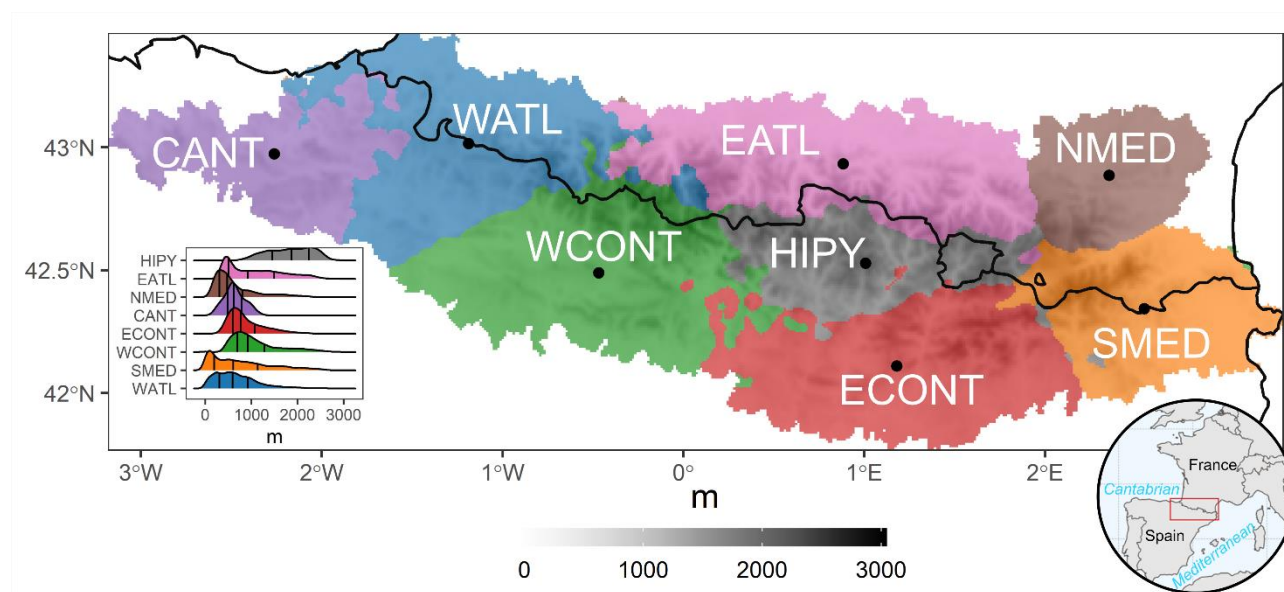
2.2 Regionalization

The Pyrenees constitute a mountainous system presenting high climatic variability, which can be summarized quite easily in order to explain the major part of the compound behavior of Dry-Hot events. In this sense, the authors consider that many regions are of no particular interest for the present analysis, because situations of long dry spells and extremely hot temperatures, for instance, display a practically identical synoptic behavior pattern throughout the region. For example, a subtropical ridge produces a dry environment and above-average temperatures throughout the Pyrenees (Lemus-Canovas et al., 2019a). This does not occur when spatial patterns of precipitation are investigated, because spatial variability is much greater. Interestingly, with northern advection in this area, precipitation can be abundant on the Atlantic and northern slopes, but scarce or non-existent on the southern slopes (Lemus-Canovas et al., 2018). This variability therefore differs depending on the variables analyzed.

The use of clustering techniques is very common in the creation of regions of climate variables. For example, Carvalho et al., (2016) regionalized temperature and precipitation in Europe; Carro-Calvo et al., (2017) performed similar tasks for tropospheric ozone; and more recently, Lemus-Canovas et al., (2019b) employed these techniques by combining precipitation with circulation types to establish rainfall regions in the Alps. In the present paper we conducted a combined regionalization of temperature and precipitation, (as both variables constitute the basis of Dry-Hot events) by applying the k-means algorithm to the daily series of temperature and rainfall (normalized) of spring and summer. In order to obtain a robust regionalization, a maximum of 100 iterations was established. To decide the optimal number of clusters, we



115 performed an iteration from $k = 2$ to $k=15$, obtaining 14 different classifications (see Fig. S1 in the Supplement). Total variance can be explained by the increase in k clusters, as shown in the Scree test (Cattell, 1966) in Fig. S2. Such a representation shows two points, – $k = 5$ (40%) and $k = 8$ (48%) – which could be considered as a "slope change", and therefore possible delimiters of the number of regions. Despite the use of the Scree test, the decision is subjective, and a compromise is therefore needed between the degree of complexity and the descriptive capacity of the regionalization (Carro-Calvo et al., 2017). Consequently, we decided to use 8 clusters, which explain 48% of the variance (Fig. S2).



120

Figure 1. Regionalization obtained with the k-means method. From left to right: CANT: Cantabrian; WATL: West Atlantic; WCONT: West Continental; EATL: East Atlantic; HIPY: High Pyrenees; ECONT: East Continental; NMED: North Mediterranean; SMED: South Mediterranean. In the bottom left-hand corner, the elevation probability density curves (m) are shown for each region. The vertical lines indicate the 25th 50th and 75th quantiles. The elevation base map was generated using the data provided by the Shuttle Radar Topography Mission (SRTM).

125

For the construction of the regionalized series, the daily values of all cells were averaged in order to work with a series that is smoother than if the centroids were used. The main reason for working with averaged regional series was to avoid the downscaling process in the application of the bias correction method. Thus, inflation and modification of the trend represented by the climate model (Maraun 2013) were avoided, among other undesirable effects. This and other aspects relating to the application of the bias correction are explained in section 2.4.

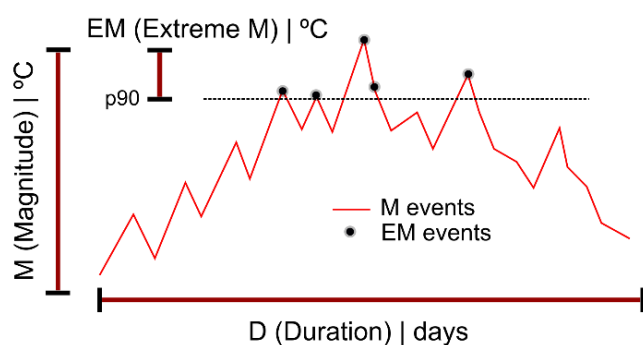
130



2.3 Event definition

As previously stated, the Dry-Hot events are characterized by means of the following dimensions: duration (D), magnitude (M) and extreme magnitude (EM), corresponding to the spring months: March, April and May (MAM); and to the summer months: June, July and August (JJA); both seasons are analyzed independently. D is defined as the number of consecutive days on which precipitation is below 1 mm (Fig. 2). This threshold was chosen to be consistent with previous studies (Orlowsky and Seneviratne 2012; Donat et al., 2013; Lehtonen et al., 2014; Manning et al., 2019), as well as to avoid the drizzle effect, which systematically causes climate models to overestimate precipitation (Gutowski et al., 2003).

To ensure that independent and extreme spells were obtained, those with a duration greater than the 90th percentile were selected annually. Additionally, M was defined as the maximum temperature values (T_x) observed during the period in which D occurred, while EM differs from M on providing T_x values greater than the 90th percentile. A schematic summary of the variables studied is presented in Figure 2.



Acronym	Definition
D	Extreme dry spell length ($> 90^{\text{th}}$ percentile) per year
EM	Extreme maximum temperature ($> 90^{\text{th}}$ percentile) during a D event
M	Maximum temperature during a D event

Figure 2. Scheme of the role of each variable in the analysis. D indicates the duration of the dry event ($> p90$, annually); M are all the days with a maximum temperature (T_x) of the event D ; EM are the days with a $T_x > p90$ within D .

Analyzing the EM subset enables us to characterize the greater risk of the simultaneous occurrence of both variables: D and EM , which in turn may significantly increase the risk of wildfires, for example. To estimate the trend of the events and to assess the statistical significance of these trends we employed Sen's slope (Sen, 1968) and Mann-Kendall's non-parametric test (Mann, 1945).



150 **2.4 Bias correction and evaluation**

Bias correction techniques are commonly used to correct the data simulated by the RCM by means of the observed data; among these techniques, the most popular and widely used is Quantile Mapping (QM). Bias correction by QM is frequently used to downscale simulations at the station level or in high-resolution grid boxes; however, it induces inflation problems in the corrected series (Maraun, 2013) and is unable to generate daily subgrid variability (Maraun et al., 2017). The above
155 mentioned issues tend to be exacerbated in mountain areas, where many local processes may not be represented following the QM process (Maraun and Widmann, 2018).

In the present study 1) we aggregated all observed data computed from D, M and EM at each regional level (Fig. 3), calculating the mean of such variables from the grid cells belonging to each of the regions of the study area; 2) we extracted the time series from the cell closest to the centroid of each region for each RCM (table 1); 3) we applied the Empirical QM
160 method (EQM), which estimates the values of the empirical cumulative distribution function (CDF) of the observed and modelled time series for each quantile (Gudmundsson et al., 2012) of the variables D, M and EM.

The bias correction was evaluated by means of a 5-fold cross validation of 7 years (4 folds for adjustment and 1-fold for validation). Cross-validation should not be applied on validating free-running climate simulations against observed series, as the climate models are temporarily stochastic and could induce severe errors in the assessment process of the daily series
165 (Maraun and Widmann, 2018). However, herein we work with annually aggregated data of the variables, D, M and EM (see section 2.3), where the RCM is expected to be able to reflect the seasonality component and trend.

The evaluation of the EQM - which is not intended to focus on the individual performance of each model, but rather on the overall result - is based on estimating the bias both in magnitude and in trend. It is assumed that once the EQM is applied, the bias in the trend of the respective variables (D, M and EM) should be lower between the bias-corrected data and the raw
170 RCM, than between the observed data and the bias-corrected data because, as described below, it is the RCM that is capable of modelling the future trend based on the drivers of future climate.

To estimate the bias in the trend, the decadal trend was computed by means of Sen's slope. Furthermore, we also estimated the bias in the variability between the observed data and the bias-corrected data by means of the coefficient of variation (CV).

175 The procedure discussed in this section, which involves applying the regional average of observations, is intended to avoid, among other problems, modification of the trend by the EQM (Cannon et al., 2015), which should be more similar to the trend projected by the RCMs than to the observed data, because the future climate will be driven by factors other than the current ones, which are measured by the RCMs.

3. Characterization of the variables underlying the compound event and of the role they play in potential risks

180 Extremely long dry spells (D) have a main north-south pattern in which the northernmost areas present extreme D values of fewer than 20 days in spring and summer, and the southernmost areas provide values that can exceed 70 days, mainly in



185 summer (Fig. 3). A second spatial pattern enabled the Atlantic and Mediterranean coastal areas to be differentiated. The former area presented the lowest number of extreme spells throughout the study area in spring and summer. On the other hand, the Mediterranean area showed a very high number of extreme dry spells, especially in summer, when these lasted on average up to 90 days. These spatial patterns showed that, despite the small size of the study area, the D patterns are very diverse.

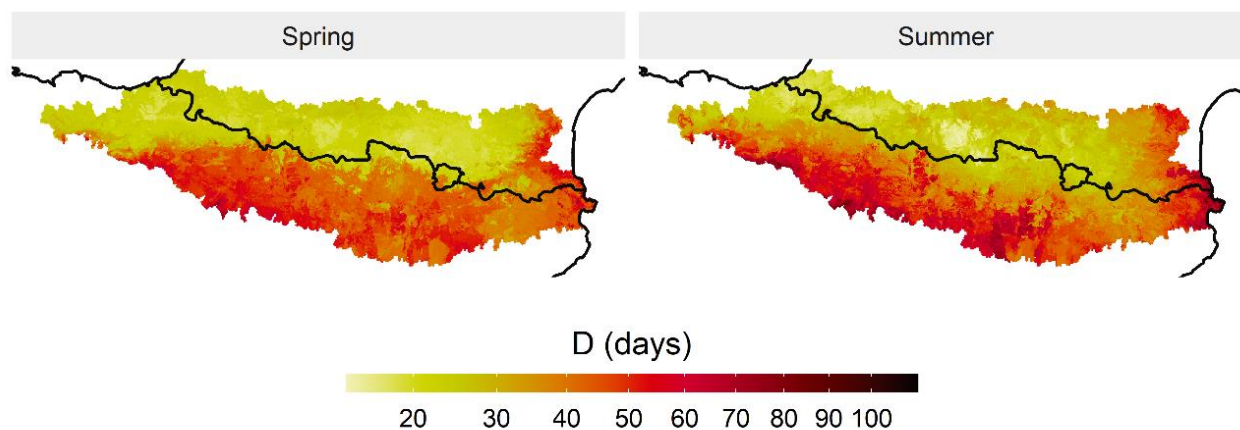
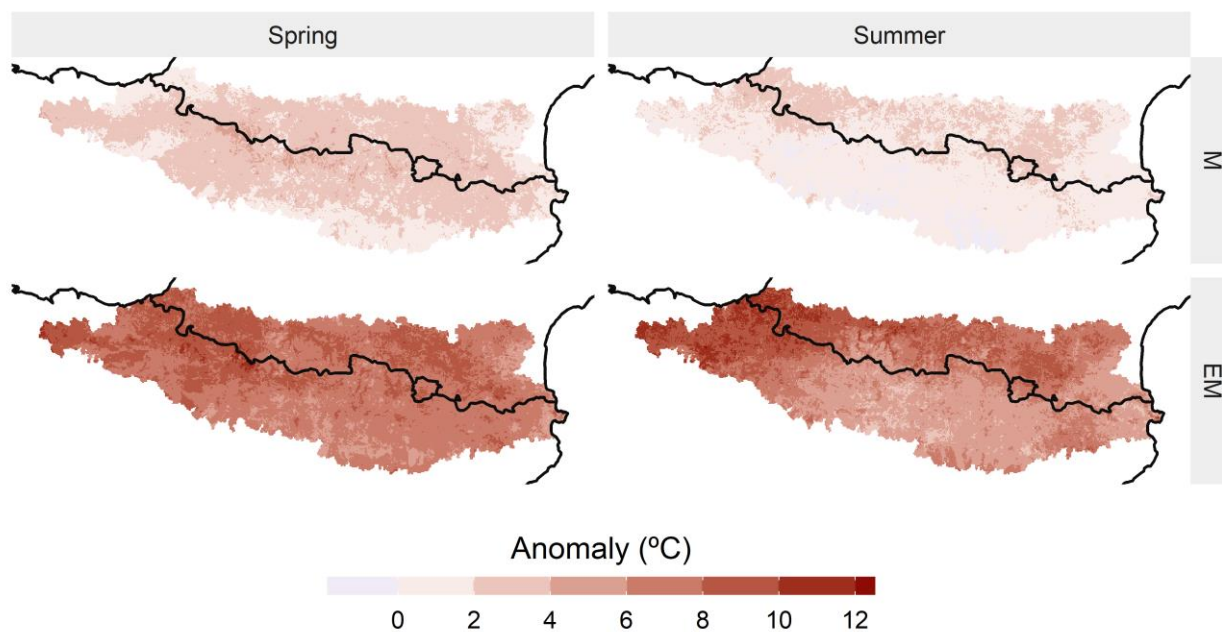


Figure 3. Averaged extremely long dry spells (>p90) for spring and summer during 1981-2015 period.

190 However, the present paper did not only focus upon variable D – we also examined the combination of this variable and extremely long dry periods. In this sense, it is important to emphasize the difference between analyzing only the Tx values of the days comprising D, which we called M, and analyzing the Tx values >90th percentile (EM). This difference is illustrated in the Tx anomalies of both periods (Fig. 4).



195 **Figure 4. Average maximum temperature (T_x) anomaly for M and EM events and for spring and summer. The average anomaly recorded for EM events is significantly higher.**

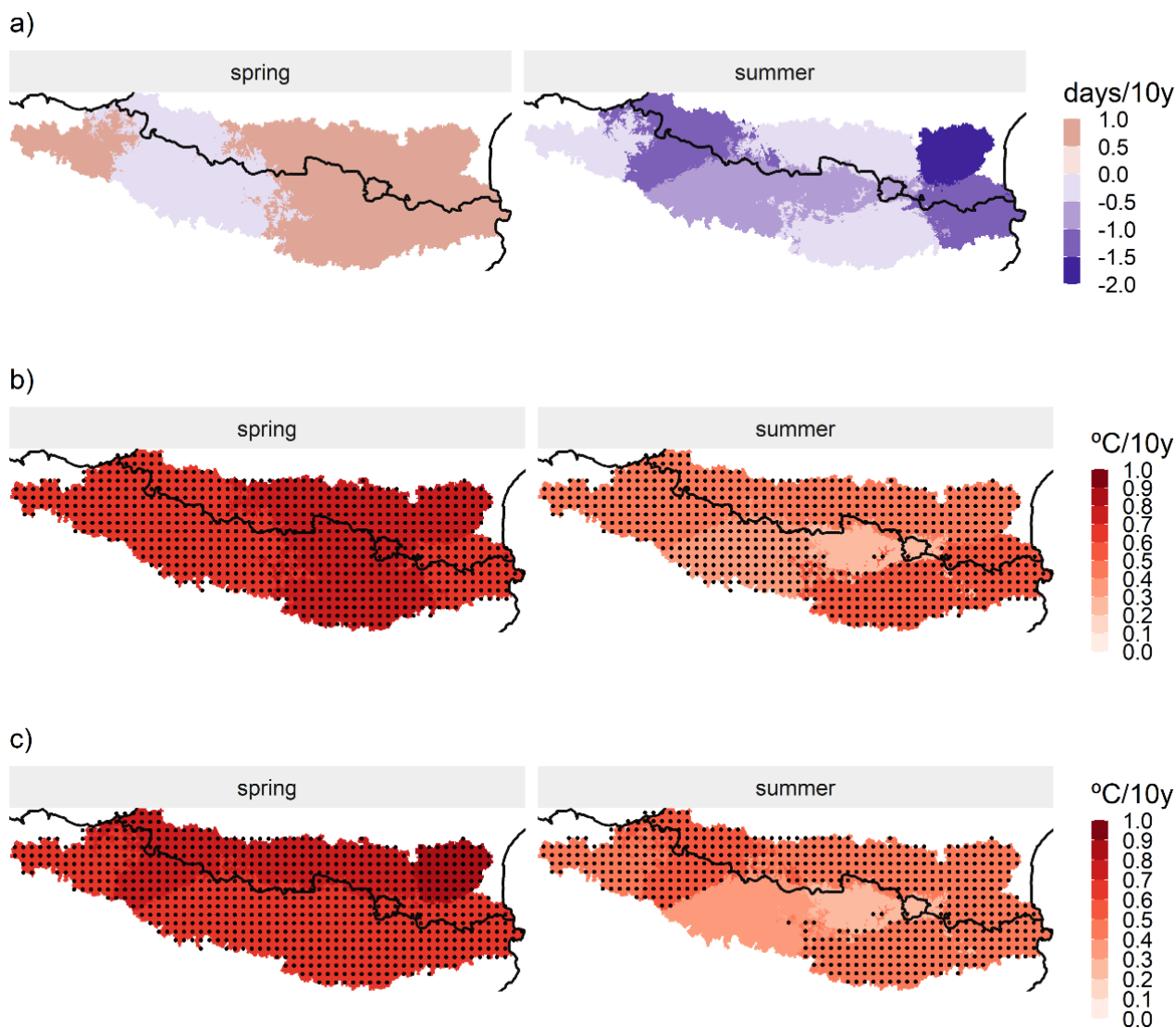
Such anomalies are clearly more positive on examining the EM variable with respect to M. This indicated that the average magnitude of days with extreme temperature within extreme dry spells was, in some cases, more than 10 times greater than the average thermal magnitude of all days contained in the dry spell. In addition, we observed a clearly opposite spatial pattern to that in Fig. 4, in which the most extreme positive anomalies were reached in the areas exhibiting the lowest number of extreme dry spells (Fig. 3). This was mainly due to the fact that in these areas the number of days with precipitation (and therefore with a moderate T_x) is very high by default (Lemus-Canovas et al., 2019a). Consequently, although the spells are short, they give rise to an extremely positive thermal anomaly, mainly on the hottest days of the spell (See EM for Summer in Fig. 4). In contrast, in the south of the Pyrenees, most days present hardly any precipitation, especially in summer, and dry spells and a positive thermal anomaly are therefore not synonymous (see M for summer in Fig. 4). A similar explanation can be found in the seasonal differences: summer is the dry season in most of the study area, which usually presents high thermal values and no precipitation; consequently, thermal anomalies of M and EM are generally lower than those observed in spring.

Before analyzing the future projection of the variables D, M and EM, we reviewed the observed trends of such variables for each region and season. In the case of D (Fig. 5a), a non-significant trend was observed (p -value ≤ 0.05) at the 95% confidence level. A high intrannual variability of the duration of extreme dry spells was detected.

210



This did not occur on assessing the EM and M trends (Fig. 5c,b, respectively), as both variables displayed a tendency to increase. This trend presented a higher slope in the spring and in the case of the EM. Indeed, the annual values of EM for spring and summer were almost all positive, whilst this was not the case on evaluating only M. At an intra-regional level, the main differences were observed in summer for EM, when the Mediterranean regions NMED and SMED accounted for a higher slope than the other regions. On the contrary, in spring growth was practically the same for all regions for EM and M. Remarkably, the HIPY region did not show a significant increase in summer for EM and M for a p-value ≤ 0.05 .

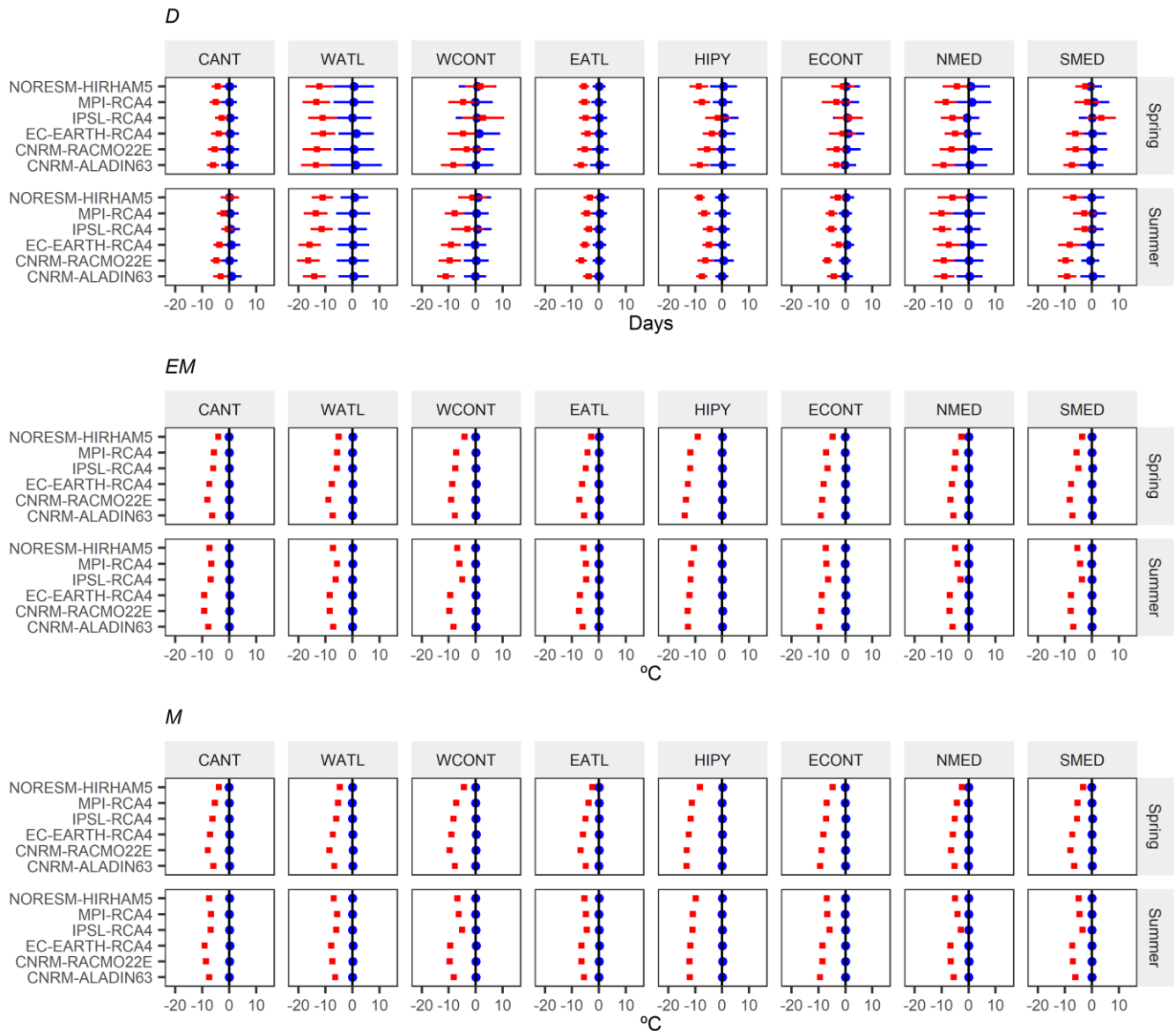


220 **Figure 5.** 10-years trend (Sen's slope) for a) extreme dry spell events (D), b) for maximum temperature events within the dry event (M) and for c) extreme maximum temperature events within the dry event (EM); for the spring and summer seasons and for all regions of the study area. The stippling shows statistically significant regions at the 95% confidence level.



4. Assessing the reliability of the bias-corrected projections

225 We evaluated the EQM in order to estimate the bias in D, EM and M (Fig. 6), as well as the bias in trend (Fig. 7), assuming that this should be lower between the raw RCM and the bias-corrected data of the RCM, than between the observed data and bias-corrected data of the RCM. We also estimated the bias in the variability between the observed data and the bias-corrected data (Fig. S3).



230 **Figure 6. Biases for each variable (D, EM and M), region, model, and season. Blue points refer to the bias corrected model, and red squares refer to the raw model.**

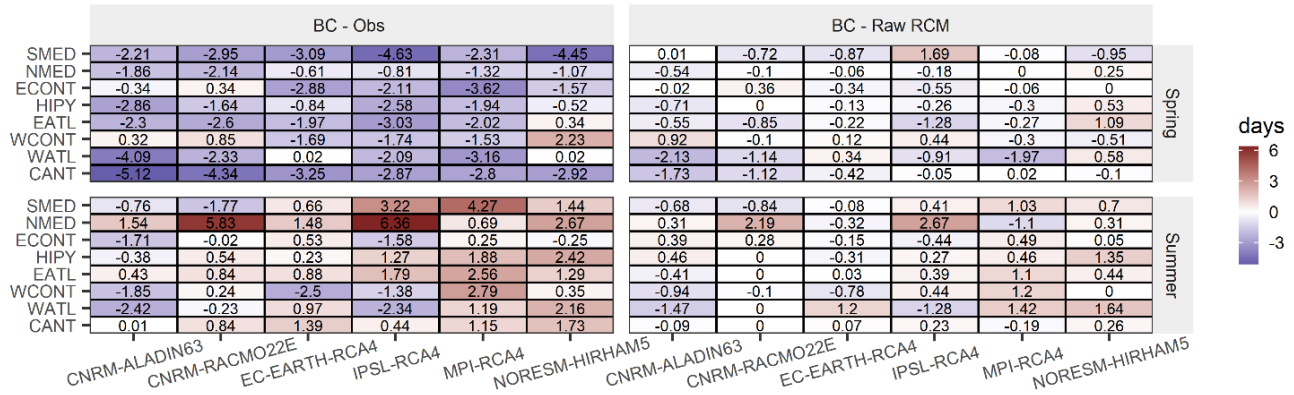


As in the case of Rajczak et al. (2016), the results showed that the EQM was capable of adjusting the mean bias of the variable D, although it showed a high spread. RCMs tend to overestimate wet days, and in the opposite case, they greatly underestimate the dry days, an issue that can be resolved by EQM (Fig.6). The bias of the variables M and EM was also satisfactorily corrected, with a low degree of deviation. The results of the bias in magnitude was satisfactory in all regions. Analysis of the bias in the trend also provided satisfactory results (Fig. 7). For all variables, in particular EM and M, the bias was clearly lower between the BC RCM and the raw RCM, which indicated that the trend of the RCM was respected on applying the EQM. In the case of D, the bias was higher and more variable in all models. However, we also observed a decrease in the bias between the BC RCM and the raw RCM in relation to the BC and the observed data.

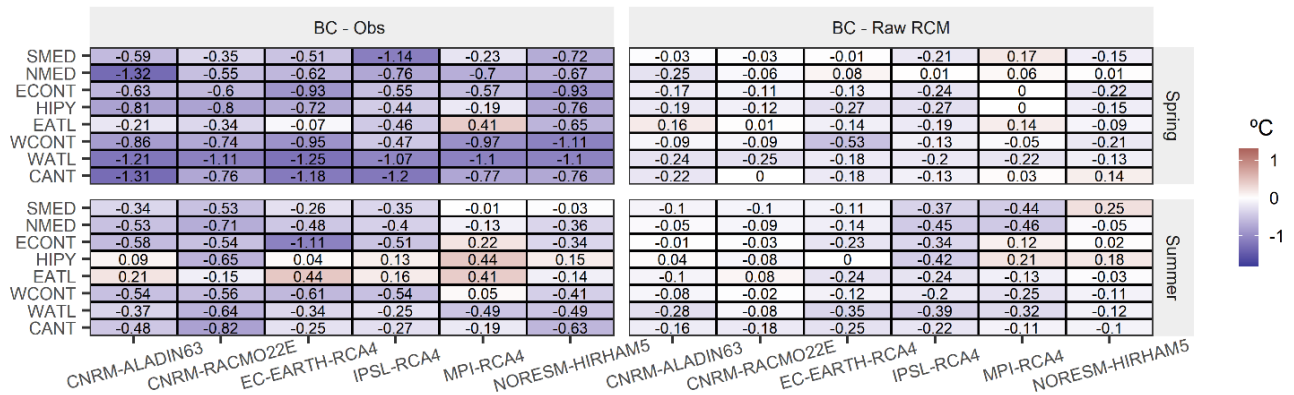
235
240



D



EM



M



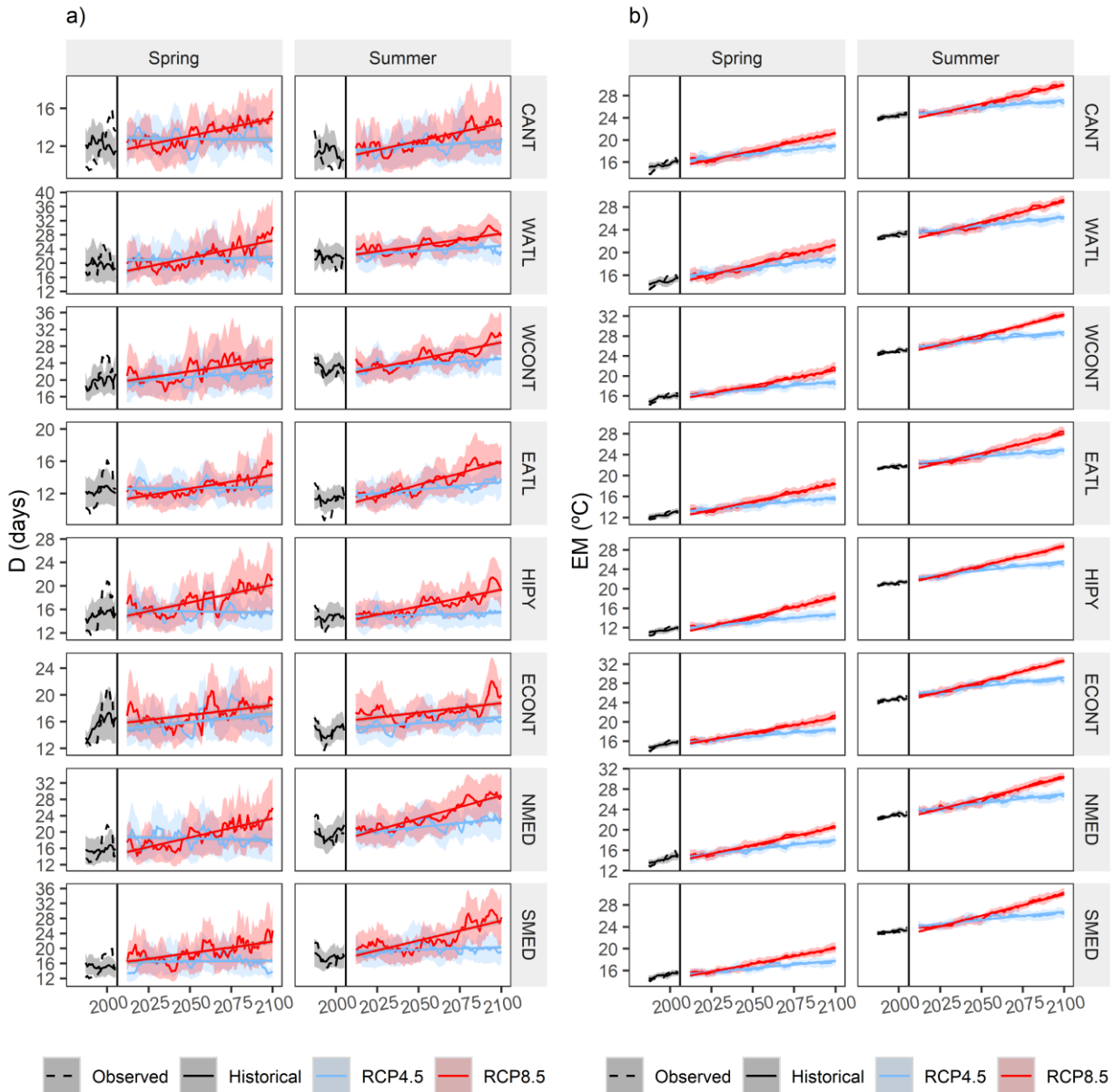
Figure 7. Biases in the trend for each variable (D, EM and M), region, model, and season. The panels on the left show the bias between the bias-corrected model (BC) and the observed data (Obs), while the panels on the right show the bias between the bias-corrected data and the uncorrected climate model (Raw RCM).



245 Finally, and in accordance with the results shown above, evaluation of the bias in the variability (Fig. S3) revealed that this was higher in D than in EM or M.

5. future changes in the magnitude of intervention of the variables underlying the compound event

250 The regional projections showed an increase in the duration of D events (Fig. 8a); these were only abundant in the case of the scenario of high greenhouse emissions (RCP8.5) and were consistent across all regions. However, the scenario projected by the RCP4.5 contrasts greatly with the previous one. In a moderate scenario, no region, with the exception of the continental regions WCONT and ECONT, showed any statistical significance in the duration of D events during spring. In summer, and under this same scenario, there was a statistically significant trend towards an increase in D events, but with a much flatter slope, especially in the HIPY and SMED regions.

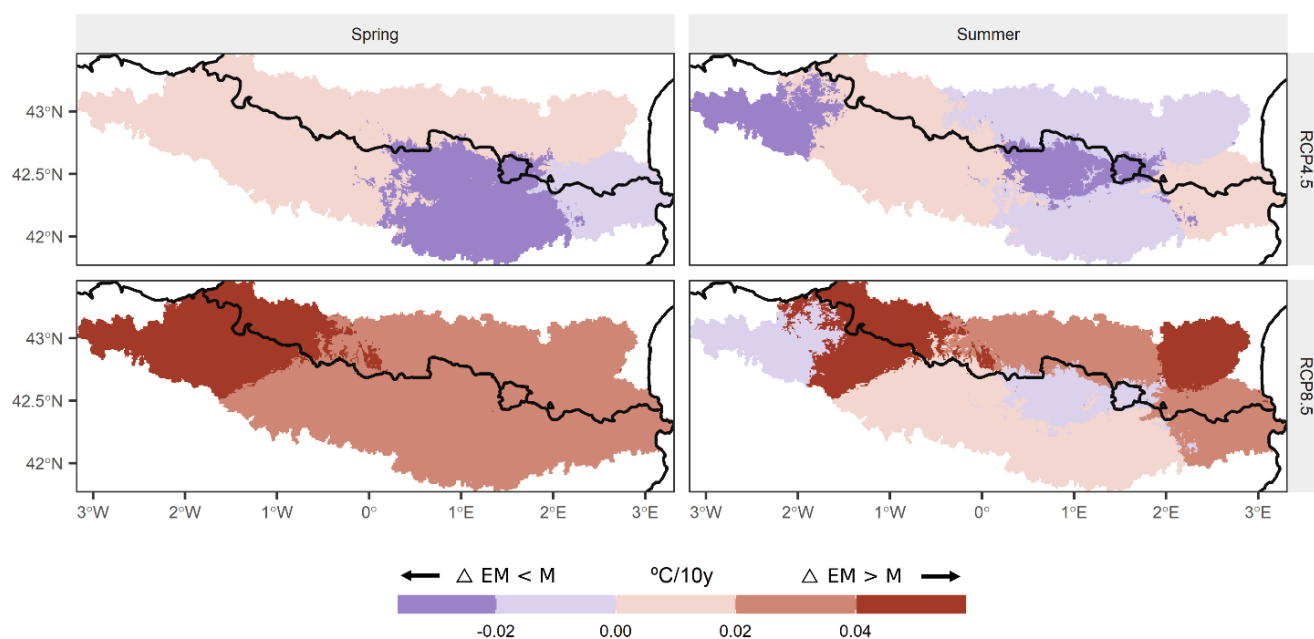


255 **Figure 8. Observed period and historical (1981-2005) and future (2006-2100) projections (7 year-moving average) of the events of a) D and b) EM for an intermediate (RCP4.5) and extreme (RCP8.5) scenarios for all regions and for the spring and summer seasons. The curves show the average value of all models, while the shaded area indicates the standard deviation of the models for each year**

260 In the case of the hot extremes (EM), the previously detected increase was evident under both scenarios (Fig. 8b). However, special attention should be paid to the greater increase in EM in relation to M (Fig. 9).



Moreover, the rate of warming during the hot extremes was variable albeit more consistent in a high-emission scenario (RCP8.5) (Fig. 9). Interestingly, under this scenario and during the spring, the EM trend was above M throughout the study area, with particular incidence in the CANT and WATL regions. In summer, the increase in EM was greater than that in M in the Mediterranean regions, especially in NMED, as well as along most of the northern slope of the Pyrenees (EATL and WATL). In the intermediate scenario, there was greater equilibrium between the EM and M trends. The HIPY region is of special interest; it presents the highest average elevation in the study area, with several glaciers and a multitude of snow-capped mountains remaining, due to its being the region exhibiting the lowest overall EM trend.



270 **Figure 9. Projected difference between the trends of M events and of EM events. Positive values indicate a higher positive trend in EM events than in M events. Conversely, negative values show a higher trend in M events than in EM events.**

It is of particular interest to analyze these D and EM events jointly to ascertain whether the compound risk of these two variables will be equally distributed or whether each of the two variables will have a different weighting in the joint event. This evaluation is shown in Figure 10 for the CANT and NMED dipole regions, where the multivariate coordinates of the anomalies of events D and EM are shown; these are divided into three periods: (2011-2040, 2041-2070 and 2071-2100) for both seasons and both emission scenarios. On the one hand, the displacement along the Y axis enabled the increase in the duration dimension (D) in the compound event to be evaluated. On the other hand, the displacement along the X axis indicated an increase in the thermal anomaly and consequently, greater risk posed by the magnitude dimension (EM). In the case of the CANT region, the average value of the bivariate distribution of each spring and summer period projected by the RCP4.5 clearly indicated that the increase in the compound risk was caused by an increase in extreme magnitude (EM), i.e.



by the thermal increase, as opposed to an increase in the duration of such events (D). The same assessment can be extrapolated to the NMED region for the spring in a RCP4.5 scenario. Nonetheless, in the case of summer for this same scenario, a small increase in the duration component was observed. In the RCP8.5 scenario, a very considerable increase in risk was perceived as a result of the increased weight of the magnitude, especially in the last two periods in both seasons and regions. The increase in the D dimension continued to be very weak for the CANT region, regardless of the season analyzed. On the other hand, in the NMED region, there was a remarkable increase in dimension D, which rose by an average of 10 days (summer, 2071-2100) with respect to the historical average (1981-2005). In this case, we detected that the increase in the compound risk occurred in both dimensions (up to 7°C in summer), thus implying a much higher risk than in the CANT dipole region.

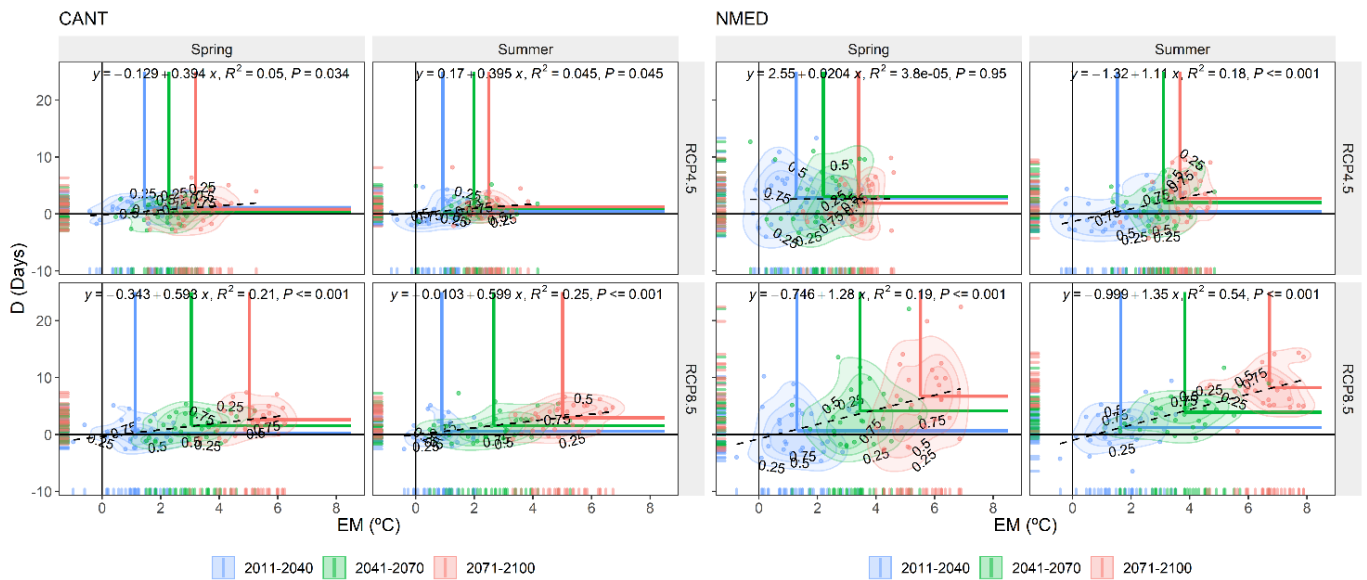
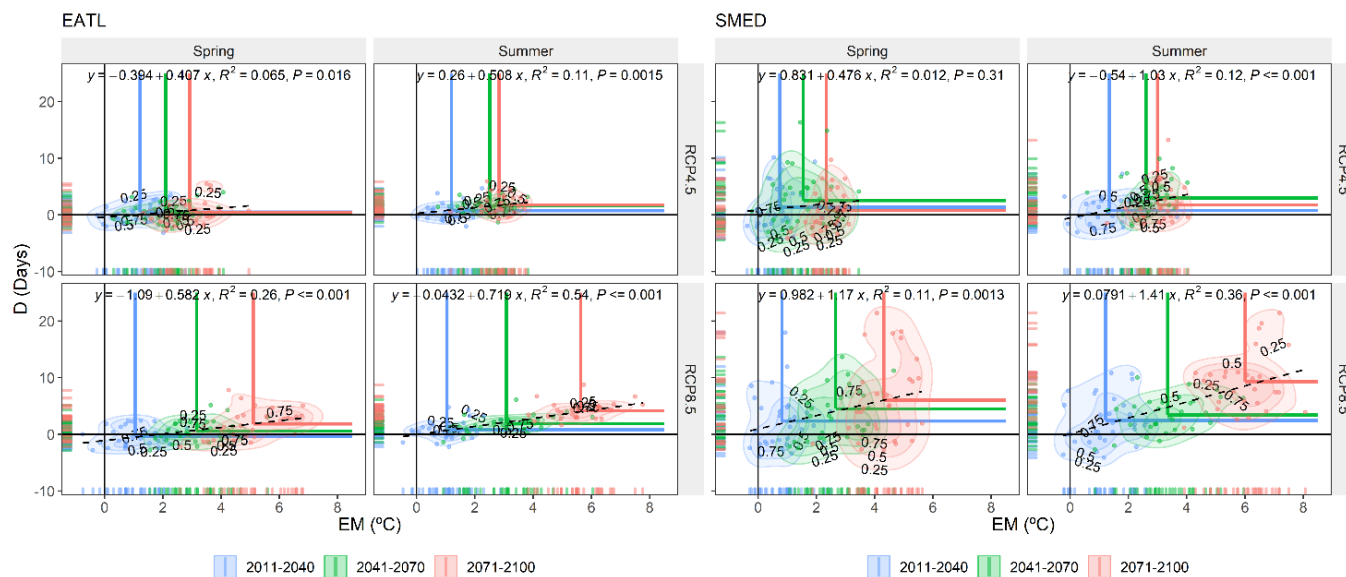


Figure 10. Bivariate probability density functions (scaled from 0 to 1) of D and EM for the three future periods (2011-2040, 2041-2070 and 2071-2100) and for the two emission and seasonal scenarios for the CANT and NMED regions. The intersection of the blue, green and red horizontal and vertical lines indicates the mean value of the bivariate distribution for each period.

A very similar phenomenon was detected between the EATL region, conditioned by a more oceanic and temperate climate, and the SMED region, with drier and warmer conditions (Fig. 11). Although in RCP4.5 the compound risk increased with a rise in extreme temperatures (EM) in both seasons of the year, in an extreme scenario (RCP8.5), and mainly in the SMED region, the compound risk increased as a result of an increase in both dimensions (D and EM).



300 Figure 11. Same as Fig. 11 but for EATL and SMED.



These results were summarized in Figure 12, which shows the future patterns of Dry-Hot compound events according to the D and EM variables of the CANT and NMED regions, which act as a dipole in the study area. Each season and emission scenario present a different pattern, summarized below:

- 305 • **Spring | RCP4.5:** Increase in one-dimensional compound risk based on (extreme) magnitude. No major shifts between dipole regions.
- **Summer | RCP4.5:** Increase in one-dimensional compound risk mainly based on (extreme) magnitude. Although a greater increase in EM was quantified in the Mediterranean and continental regions (see Fig. 10 and Fig. 11), a small increase was also reported in the second dimension when the duration of the dry event showed an increase.
- 310 • **Spring | RCP8.5:** Increase in risk resulting from a certain two-dimensional component, particularly in the Mediterranean and continental regions. The increase in (extreme) magnitude was slightly greater in the Mediterranean and continental regions. There was a big increase in the second dimension in the above mentioned regions, and a small one in the dipole regions.
- 315 • **Summer | RCP8.5:** Increase in two-dimensional compound risk in Mediterranean areas, greater than the previous pattern. The increase in the opposite regions was practically the same as the Spring | RCP8.5 pattern, mainly in the EM dimension. The increase in EM in the last period in the Mediterranean regions was the highest of the four patterns described.

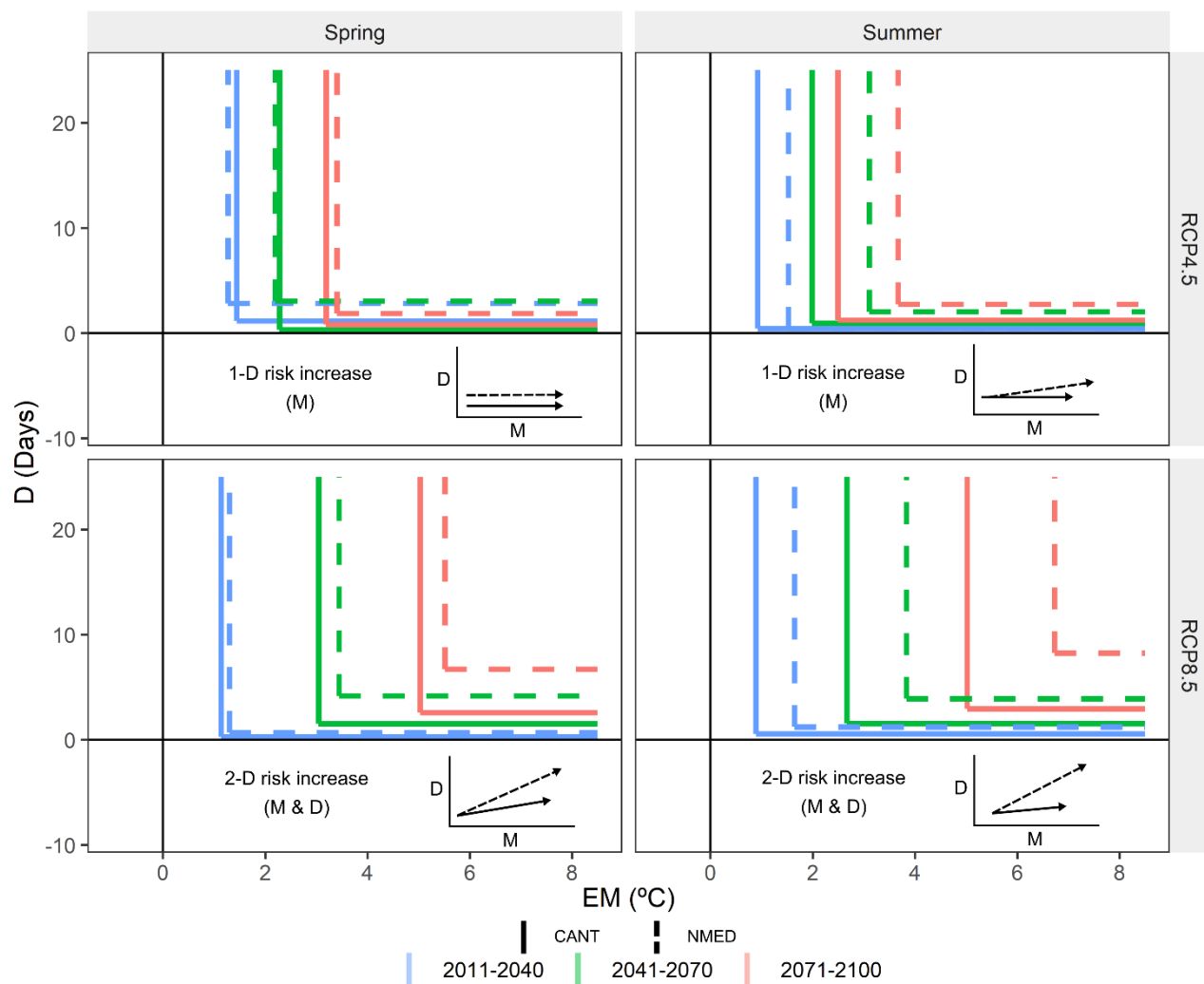


Figure 12. Diagram of the drivers of the three future periods (2011-2040, 2041-2070 and 2071-2100) of the compound event for D and EM in the CANT (solid line) and NMED (dashed line) regions, which acted as a dipole in the study area.



320 The remaining regions shown in the supplementary document were at the intermediate stages of those described herein (Fig. S4 and Fig. S5). However, the WATL region, which is adjacent to the CANT region, was influenced by both climates (Atlantic and Mediterranean) and therefore did not reflect a similar behavior pattern to that of the CANT region (see Fig. 1 to verify the heterogeneity of this region).

6. Discussion

325 The results of the present research reveal that up to the present there has been a general increase in the compound risk of Dry-Hot events due to an increase in the thermal component; thus, the duration dimension is excluded, as pointed out in various recent studies (Hao et al., 2018; Manning et al., 2019). A significant finding of our study indicates that there will be a significant increase in the future compound risk in relation both to the magnitude dimension (extreme temperature) and the duration dimension (duration of extreme dry event). Therefore, it was estimated that in the future the compound event will exhibit a more balanced distribution between the two dimensions, with the D dimension gaining prominence. Polade et al., (2014) showed that the areas in which a greater increase in dry days is expected under a RCP8.5 scenario are the western Mediterranean and the eastern Atlantic, at approximately latitudes 35°N and 55°N, in accordance with the findings of the present study.

330 Nonetheless, there are conflicting opinions regarding whether the observed warming is inducing an increase in the length of dry spells, as noted by Ye and Fetzer (2019) in Russia, or whether, as observed by Trenberth et al., (2014), the warming does not prolong the dry event, but that the warming itself may augment the intensity of the episode due to the effect of thermal magnitude. The authors consider that the observed warming has not caused longer-lasting droughts in the area of the Pyrenees, which does not correspond with the findings of Ye and Fetzer (2019). Furthermore, even under an intermediate emissions scenario (RCP4.5), there is no evidence of increasingly longer dry spells, despite a significant rise in temperature. 340 Consequently, the authors do not support the idea that a thermal increase is directly related to longer dry periods. This greater duration of dry spells in the most extreme emission scenarios may be due to northward shifting of the subtropical anticyclone belt (Gillett and Stott 2009) as a consequence of the expansion of the Hadley cell in response to global warming (Lu et al., 2007). There is a need for further research in order to understand the future role of the subtropical anticyclone belt and variations therein, and how these affect increases or decreases in compound events.

345 7. Conclusions

The risk posed by the simultaneous occurrence of extremely dry and hot events is analyzed for the first time in the Pyrenees, which is a very fragile area as a result of its altitude and transition latitude between the temperate and subtropical climates. Moreover, 59% of its area is covered by forests, which will become susceptible to severe wildfires if climatic conditions are unfavorable during the following years. We extracted the following main findings from the present study:



- 350
- The results for the observed period (1981-2015) showed a generalized increase in the thermal extremes (EM) within the extreme dry spells (D), with no increase in the duration of these spells. This showed that to date the compound risk has only augmented in one dimension: Extreme magnitude (EM) and by default, magnitude (M).
 - As regards the results obtained from future projections, it is essential that an intermediate emission scenario (RCP4.5) not be exceeded, as this serves to prevent the D dimension (duration) of such events from increasing. The

355

 - In a high-emission scenario (RCP8.5), the increased risk of the compound event would be a consequence of an increase in both the extreme magnitude (EM) and the duration (D) dimensions. In addition, and within this context, the thermal increase in extremely hot days (EM) during the dry event (D) is greater than the thermal increase in the set of days (M) comprising the dry event (D).
- 360
- Finally, and as a general conclusion, the present study reveals a potential increase in the environmental risk in the Pyrenees (fires, crop yield losses, effects on biodiversity, water resources, etc.) resulting from more frequent compound events involving long dry periods and extreme temperatures during these periods, mainly in the Pyrenean Mediterranean area and in the south of the Pyrenees. For the moment, the high-altitude regions and those with an oceanic climate could be affected to a lesser extent, although under a scenario of high emissions they will also suffer a greater risk in the 2D.
- 365
- There exists a need to study whether, for example, wildfires are observed during such extremely hot intervals within these very long dry periods, in order to prepare this area to deal with large wildfires.

Acknowledgements

The present research was conducted within the framework of the Climatology Group of the University of Barcelona (2017 SGR 1362, Catalan Government), and the CLICES project (CGL2017-83866-C3-2-R, AEI/FEDER, UE). We wish to thank

370

Dr. Cuadrat and Dr. Serrano-Notivoli for the CLIMPY project database. M.L-C was awarded a pre-doctoral FPU Grant (FPU2017/02166) from the Spanish Ministry of Science, Innovation and Universities. The authors declare no conflict of interest.

Data availability

CLIMPY database is available from: https://zenodo.org/record/3611127#.X_NxyRaCFPY. EURO-CORDEX projections

375

are available from <https://cds.climate.copernicus.eu/cdsapp#!/dataset/projections-cordex-domains-single-levels?tab=overview>.



Author contribution

380 M.L-C and J.A L-B: Conceptualization. ML-C: Methodology, Data curation, Writing-Original draft preparation. JA.L-B:
Supervision

Competing Interests

The authors declare that they have no conflict of interest.

References

- 385 Camarero, J. J.: The Multiple Factors Explaining Decline in Mountain Forests: Historical Logging and Warming-Related
Drought Stress is Causing Silver-Fir Dieback in the Aragón Pyrenees, in *Advances in Global Change Research.*, 2017.
- Cannon, A. J., Sobie, S. R. and Murdock, T. Q.: Bias correction of GCM precipitation by quantile mapping: How well do
methods preserve changes in quantiles and extremes?, *J. Clim.*, doi:10.1175/JCLI-D-14-00754.1, 2015.
- Carvalho, M. J., Melo-Gonçalves, P., Teixeira, J. C. and Rocha, A.: Regionalization of Europe based on a K-Means Cluster
Analysis of the climate change of temperatures and precipitation, *Phys. Chem. Earth*, doi:10.1016/j.pce.2016.05.001, 2016.
- 390 Cattell, R. B.: The scree test for the number of factors, *Multivariate Behav. Res.*, doi:10.1207/s15327906mbr0102_10, 1966.
- Cuadrat, J. M., Serrano-Notivoli, R., Tejedor, E., Saz, M. Á., Prohom, M., Cunillera, J., Llabrés, A., Trapero, L., Pons, M.,
López-Moreno, J. I., Copons, R., Gascoïn, S., Luna, Y., Rodríguez, E., Ramos, P., Amblar, P. and Soubeyroux, J.-M.:
CLIMPY: Climate of the Pyrenees, , doi:10.5281/ZENODO.3611127, 2020.
- De Luca, P., Messori, G., Faranda, D., Ward, P. J. and Coumou, D.: Compound Hot-Dry and Cold-Wet Dynamical Extremes
395 Over the Mediterranean, *Earth Syst. Dyn. Discuss.*, 2020, 1–24, doi:10.5194/esd-2020-21, 2020.
- Diffenbaugh, N. S. and Ashfaq, M.: Intensification of hot extremes in the United States, *Geophys. Res. Lett.*,
doi:10.1029/2010GL043888, 2010.
- Donat, M. G., Alexander, L. V., Yang, H., Durre, I., Vose, R., Dunn, R. J. H., Willett, K. M., Aguilar, E., Brunet, M.,
Caesar, J., Hewitson, B., Jack, C., Klein Tank, A. M. G., Kruger, A. C., Marengo, J., Peterson, T. C., Renom, M., Oria
400 Rojas, C., Rusticucci, M., Salinger, J., Elrayah, A. S., Sekele, S. S., Srivastava, A. K., Trewin, B., Villarroyel, C., Vincent, L.
A., Zhai, P., Zhang, X. and Kitching, S.: Updated analyses of temperature and precipitation extreme indices since the
beginning of the twentieth century: The HadEX2 dataset, *J. Geophys. Res. Atmos.*, doi:10.1002/jgrd.50150, 2013.
- Fonseca, D., Carvalho, M. J., Marta-Almeida, M., Melo-Gonçalves, P. and Rocha, A.: Recent trends of extreme temperature
indices for the Iberian Peninsula, *Phys. Chem. Earth, Parts A/B/C*, 94, 66–76, doi:10.1016/j.pce.2015.12.005, 2016.
- 405 Gazol, A., Sangüesa-Barreda, G. and Camarero, J. J.: Forecasting Forest Vulnerability to Drought in Pyrenean Silver Fir
Forests Showing Dieback, *Front. For. Glob. Chang.*, doi:10.3389/ffgc.2020.00036, 2020.



- Hao, Z., Hao, F., Xia, Y., Singh, V. P. and Zhang, X.: A monitoring and prediction system for compound dry and hot events, *Environ. Res. Lett.*, doi:10.1088/1748-9326/ab4df5, 2019.
- Gillett, N. P. and Stott, P. A.: Attribution of anthropogenic influence on seasonal sea level pressure, *Geophys. Res. Lett.*,
410 doi:10.1029/2009GL041269, 2009.
- Gudmundsson, L., Bremnes, J. B., Haugen, J. E. and Engen-Skaugen, T.: Technical Note: Downscaling RCM precipitation to the station scale using statistical transformations – A comparison of methods, *Hydrol. Earth Syst. Sci.*, doi:10.5194/hess-16-3383-2012, 2012.
- Gutowski, W. J., Decker, S. G., Donavon, R. A., Pan, Z., Arritt, R. W. and Takle, E. S.: Temporal-spatial scales of observed
415 and simulated precipitation in Central U.S. climate, *J. Clim.*, doi:10.1175/1520-0442(2003)016<3841:TSSOAS>2.0.CO;2, 2003.
- Hao, Z., Hao, F., Xia, Y., Singh, V. P. and Zhang, X.: A monitoring and prediction system for compound dry and hot events, *Environ. Res. Lett.*, doi:10.1088/1748-9326/ab4df5, 2019.
- Hao, Z., Singh, V. P. and Hao, F.: Compound extremes in hydroclimatology: A review, *Water (Switzerland)*,
420 doi:10.3390/w10060718, 2018.
- Jacob, D., Petersen, J., Eggert, B., Alias, A., Christensen, O. B., Bouwer, L. M., Braun, A., Colette, A., Déqué, M., Georgievski, G., Georgopoulou, E., Gobiet, A., Menut, L., Nikulin, G., Haensler, A., Hempelmann, N., Jones, C., Keuler, K., Kovats, S., Kröner, N., Kotlarski, S., Kriegsmann, A., Martin, E., van Meijgaard, E., Moseley, C., Pfeifer, S., Preuschmann, S., Radermacher, C., Radtke, K., Rechid, D., Rounsevell, M., Samuelsson, P., Somot, S., Soussana, J. F., Teichmann, C.,
425 Valentini, R., Vautard, R., Weber, B. and Yiou, P.: EURO-CORDEX: New high-resolution climate change projections for European impact research, *Reg. Environ. Chang.*, doi:10.1007/s10113-013-0499-2, 2014.
- Lehtonen, I., Ruosteenoja, K. and Jylhä, K.: Projected changes in European extreme precipitation indices on the basis of global and regional climate model ensembles, *Int. J. Climatol.*, doi:10.1002/joc.3758, 2014.
- Lemus-Cánovas, M., Ninyerola, M., Lopez-Bustins, J. A., Manguan, S. and Garcia-Sellés, C.: A mixed application of an
430 objective synoptic classification and spatial regression models for deriving winter precipitation regimes in the Eastern Pyrenees, *Int. J. Climatol.*, doi:10.1002/joc.5948, 2018.
- Lemus-Canovas, M., Lopez-Bustins, J. A., Trapero, L. and Martin-Vide, J.: Combining circulation weather types and daily precipitation modelling to derive climatic precipitation regions in the Pyrenees, *Atmos. Res.*, 220, 181–193, doi:10.1016/j.atmosres.2019.01.018, 2019a.
- 435 Lemus-Canovas, M., Lopez-Bustins, J. A., Martin-Vide, J. and Royé, D.: synoptReg: An R package for computing a synoptic climate classification and a spatial regionalization of environmental data, *Environ. Model. Softw.*, 118, 114–119, doi:10.1016/J.ENVSOFT.2019.04.006, 2019b.
- Lu, J., Vecchi, G. A. and Reichler, T.: Expansion of the Hadley cell under global warming, *Geophys. Res. Lett.*, doi:10.1029/2006GL028443, 2007.



- 440 Lu, Y., Hu, H., Li, C. and Tian, F.: Increasing compound events of extreme hot and dry days during growing seasons of
wheat and maize in China, *Sci. Rep.*, doi:10.1038/s41598-018-34215-y, 2018.
- Mann, H. B.: Nonparametric Tests Against Trend, *Econometrica*, doi:10.2307/1907187, 1945.
- Manning, C., Widmann, M., Bevacqua, E., Van Loon, A. F., Maraun, D. and Vrac, M.: Increased probability of compound
long-duration dry and hot events in Europe during summer (1950-2013), *Environ. Res. Lett.*, doi:10.1088/1748-9326/ab23bf,
445 2019.
- Maraun, D. and Widmann, M.: The representation of location by a regional climate model in complex terrain, *Hydrol. Earth
Syst. Sci.*, doi:10.5194/hess-19-3449-2015, 2015.
- Maraun, D.: Bias correction, quantile mapping, and downscaling: Revisiting the inflation issue, *J. Clim.*, doi:10.1175/JCLI-
D-12-00821.1, 2013.
- 450 Maraun, D., Shepherd, T. G., Widmann, M., Zappa, G., Walton, D., Gutiérrez, J. M., Hagemann, S., Richter, I., Soares, P.
M. M., Hall, A. and Mearns, L. O.: Towards process-informed bias correction of climate change simulations, in *Nature
Climate Change.*, 2017.
- Maraun, D. and Widmann, M.: Statistical Downscaling and Bias Correction for Climate Research., 2018.
- Maraun, D. and Widmann, M.: Cross-validation of bias-corrected climate simulations is misleading, *Hydrol. Earth Syst. Sci.*,
455 doi:10.5194/hess-22-4867-2018, 2018.
- Martin-Vide, J. and Gomez, L.: Regionalization of peninsular Spain based on the length of dry spells, *Int. J. Climatol.*,
doi:10.1002/(SICI)1097-0088(199904)19:5<537::AID-JOC371>3.0.CO;2-X, 1999.
- Martin-Vide, J. and Gomez, L.: Regionalization of peninsular Spain based on the length of dry spells, *Int. J. Climatol.*,
doi:10.1002/(SICI)1097-0088(199904)19:5<537::AID-JOC371>3.0.CO;2-X, 1999.
- 460 Mazdiyasi, O. and AghaKouchak, A.: Substantial increase in concurrent droughts and heatwaves in the United States, *Proc.
Natl. Acad. Sci. U. S. A.*, doi:10.1073/pnas.1422945112, 2015.
- Orlowsky, B. and Seneviratne, S. I.: Elusive drought: Uncertainty in observed trends and short-and long-term CMIP5
projections, *Hydrol. Earth Syst. Sci.*, doi:10.5194/hess-17-1765-2013, 2013.
- Orlowsky, B. and Seneviratne, S. I.: Global changes in extreme events: Regional and seasonal dimension, *Clim. Change*,
465 doi:10.1007/s10584-011-0122-9, 2012.
- Polade, S. D., Pierce, D. W., Cayan, D. R., Gershunov, A. and Dettinger, M. D.: The key role of dry days in changing
regional climate and precipitation regimes, *Sci. Rep.*, doi:10.1038/srep04364, 2014.
- Rajczak, J., Kotlarski, S. and Schär, C.: Does quantile mapping of simulated precipitation correct for biases in transition
probabilities and spell lengths?, *J. Clim.*, doi:10.1175/JCLI-D-15-0162.1, 2016.
- 470 Riahi, K., Rao, S., Krey, V., Cho, C., Chirkov, V., Fischer, G., Kindermann, G., Nakicenovic, N. and Rafaj, P.: RCP 8.5-A
scenario of comparatively high greenhouse gas emissions, *Clim. Change*, doi:10.1007/s10584-011-0149-y, 2011.



- Salameh, A. A. M., Gámiz-Fortis, S. R., Castro-Díez, Y., Abu Hammad, A. and Esteban-Parra, M. J.: Spatio-temporal analysis for extreme temperature indices over the Levant region, *Int. J. Climatol.*, 39(15), 5556–5582, doi:10.1002/joc.6171, 2019.
- 475 Sen, P. K.: Estimates of the Regression Coefficient Based on Kendall's Tau, *J. Am. Stat. Assoc.*, doi:10.1080/01621459.1968.10480934, 1968.
- Serrano-Notivoli, R., Beguería, S., Saz, M. Á., Longares, L. A. and De Luis, M.: SPREAD: A high-resolution daily gridded precipitation dataset for Spain - An extreme events frequency and intensity overview, *Earth Syst. Sci. Data*, doi:10.5194/essd-9-721-2017, 2017.
- 480 Serrano-Notivoli, R., Beguería, S. and De Luis, M.: STEAD: A high-resolution daily gridded temperature dataset for Spain, *Earth Syst. Sci. Data Discuss.*, doi:10.5194/essd-2019-52, 2019.
- Sharma, S. and Mujumdar, P.: Increasing frequency and spatial extent of concurrent meteorological droughts and heatwaves in India, *Sci. Rep.*, doi:10.1038/s41598-017-15896-3, 2017.
- Singh, D., Tsiang, M., Rajaratnam, B. and Diffenbaugh, N. S.: Observed changes in extreme wet and dry spells during the
485 south Asian summer monsoon season, *Nat. Clim. Chang.*, doi:10.1038/nclimate2208, 2014.
- Trenberth, K. E., Dai, A., Van Der Schrier, G., Jones, P. D., Barichivich, J., Briffa, K. R. and Sheffield, J.: Global warming and changes in drought, *Nat. Clim. Chang.*, doi:10.1038/nclimate2067, 2014.
- Wise, M., Calvin, K., Thomson, A., Clarke, L., Bond-Lamberty, B., Sands, R., Smith, S. J., Janetos, A. and Edmonds, J.: Implications of limiting CO₂ concentrations for land use and energy, *Science* (80-.), doi:10.1126/science.1168475, 2009.
- 490 Wu, X., Hao, Z., Hao, F., Singh, V. P. and Zhang, X.: Dry-hot magnitude index: A joint indicator for compound event analysis, *Environ. Res. Lett.*, doi:10.1088/1748-9326/ab1ec7, 2019.
- Wu, X., Hao, Z., Tang, Q., Singh, V. P., Zhang, X. and Hao, F.: Projected increase in compound dry and hot events over global land areas, *Int. J. Climatol.*, doi:10.1002/joc.6626, 2020.
- Ye, H. and Fetzer, E. J.: Asymmetrical Shift Toward Longer Dry Spells Associated with Warming Temperatures During
495 Russian Summers, *Geophys. Res. Lett.*, doi:10.1029/2019GL084748, 2019.
- Zolina, O., Simmer, C., Belyaev, K., Gulev, S. K. and Koltermann, P.: Changes in the duration of European wet and dry spells during the last 60 years, *J. Clim.*, doi:10.1175/JCLI-D-11-00498.1, 2013.
- Zscheischler, J. and Seneviratne, S. I.: Dependence of drivers affects risks associated with compound events, *Sci. Adv.*, doi:10.1126/sciadv.1700263, 2017.
- 500 Zscheischler, J., Westra, S., Van Den Hurk, B. J. J. M., Seneviratne, S. I., Ward, P. J., Pitman, A., Aghakouchak, A., Bresch, D. N., Leonard, M., Wahl, T. and Zhang, X.: Future climate risk from compound events, *Nat. Clim. Chang.*, doi:10.1038/s41558-018-0156-3, 2018.